ISSN 1845–8319

LOW-FREQUENCY TYPE III RADIO BURSTS AND SOLAR ENERGETIC PARTICLE EVENTS

N. Gopalswamy[1] and P. Mäkelä[2]

[1] *NASA Goddard Space Flight Center, Greenbelt, MD 20771, USA*
[2] *The Catholic University of America, Washington, DC 20064, USA*

Abstract. Complex type III bursts at low-frequencies (<14 MHz) are thought to indicate large solar energetic particle (SEP) events. We analyzed six complex type III bursts from the same active region, one of which was not accompanied by a SEP event. This event was accompanied by a fast and wide coronal mass ejection (CME), but lacked a type II burst and an interplanetary shock. When we examined the evolution and the magnetic configuration of the active region, we did not find anything peculiar. The lowest frequency of type III emission occurred at the local plasma frequency in the vicinity of the Wind spacecraft that observed the type III, which confirms that the magnetic connectivity of the source region was good. We conclude that the lack of SEPs is due to the lack of production rather than due to poor magnetic connectivity. We also show that neither the type III burst duration nor the burst intensity was able to distinguish between SEP and non-SEP events. The lack of SEP event can be readily explained under the shock-acceleration paradigm, but not under the flare-acceleration paradigm.

Key words: coronal mass ejections - Type III radio bursts - solar energetic particle events - solar flares

1. Introduction

Complex type III bursts are long-duration ($\geq$ 15 min) bursts occurring at low frequencies originally identified by Cane et al., (1981). Large solar energetic particle (SEP) events are associated with complex type IIIs (Kahler et al., 1986; Cane et al., 2002; MacDowall et al., 2003), but the reverse has been proven to be not true by Gopalswamy and Mäkelä (2010). They investigated a complex type III burst associated with a fast and wide CME on 2004 April 9, but not associated with a type II burst, a solar energetic particle (SEP) event, or an interplanetary (IP) shock and concluded that a complex type III burst is not a sufficient condition for the occurrence of an SEP event. In this paper, we examine the magnetic connectivity and

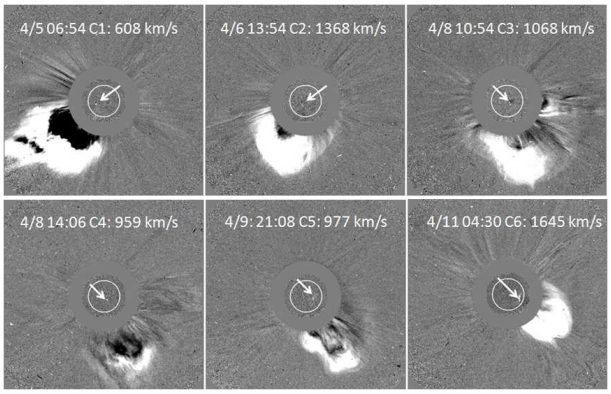

Figure 1: CMEs from AR 10588 from SOHO/LASCO. The source region (pointed by an arrow) is identified in the SOHO/EIT images superposed on the LASCO images. The general southern bias of the CMEs seems to be due to the presence of the coronal hole to the north and east of the AR (see Fig. 6).

the evolution of the source active region to see if these factors may account for the lack of SEP event. We also compare the peak and integrated flux density of the type III burst in question with other type III bursts from the same active region to see if they affect the occurrence of an SEP event.

2. Type III Bursts, CMEs, and Flares

CMEs: Since complex type III bursts are known to be associated with energetic CMEs (Gopalswamy et al., 2000), we searched for CMEs that are at least 60° wide from AR 10588 in the online CME catalog (Gopalswamy et al., 2009a): `http://cdaw.gsfc.nasa.gov/CME_list`. The catalog contains all CMEs manually identified from the images obtained by the Large Angle and Spectrometric Coronagraph (LASCO) on board the Solar and Heliospheric Observatory (SOHO) mission. Six CMEs satisfying the 60° width criterion were found on five different days: April 5, 6, 8, 9, and 11 (there were two CMEs on April 8). We denote these CMEs as C1,..., C6 for easy reference (see Fig. 1). The first and second eruptions on April 8 will be referred to as 4/8-1 and 4/8-2. The CMEs were fast (speed $\geq$ 900km/s) and wide (angular width $\geq$ 60°) except for the first one, which was wide but the speed was only $\sim$608 km/s. The two CMEs on April 8 were separated by only $\sim$3 h. The speeds, widths, and accelerations of CMEs in the sky plane projection

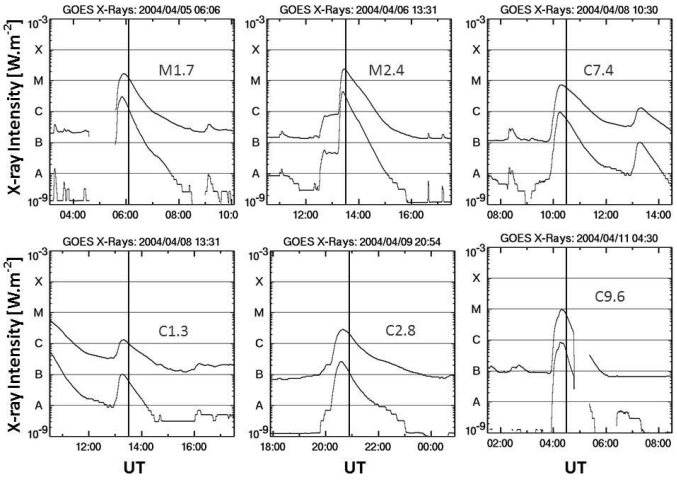

Figure 2: The GOES soft X-ray light curves of the six flares associated with the CMEs in Fig. 1. The vertical solid lines denote the times of LASCO frames showing the CMEs. There was a short data gap for the last event.

are listed in Table I.

Flares: All the six eruptions were accompanied by soft X-ray flares reported in the Solar Geophysical Data (SGD). The flares were of C and M class (see Fig. 2). The soft X-ray flare rise times (onset to peak) were in the range 15 to 27 minutes and the total flare duration ranged from 30 to 54 minutes (see Table I). In H-alpha, the flares were generally weak: the first and last were 1F flares, while the others were subflares (SF). There was no optical flare information for 4/8-2.

Radio Bursts: All the six CMEs were associated with extended type III bursts observed by the Wind/WAVES experiment (Bougeret et al., 1995) in two spectral domains: RAD1 (20 kHz–1.04 MHz) and RAD2 (1.075–13.825 MHz). We measure type III burst properties at two frequencies: 13.825 ($\sim$ 14 MHz) and 1.075 MHz ($\sim$ 1 MHz)in RAD2. Figure 3 illustrates the method of obtaining the type III burst duration for the type III burst associated with C5 shown in the RAD2 spectral domain. In Fig. 3(b,c) we show the frequency cuts at 9 and 1 MHz giving the time profile of the burst intensity. The duration of the type III burst is estimated as 25 min at 9 MHz and 28 min at 1 MHz. Clearly this is a long-duration type III burst at frequencies below 14 MHz. For this burst, there was radio interference at 14 MHz, so

Table I: Properties of CMEs, flares, and radio bursts during the six eruptions

	Date					
Property	4/5	4/6	4/8-1	4/8-2	4/9	4/11
CME identifier	C1	C2	C3	C4	C5	C6
CME first appearance (UT)	06:06:05	13:31:43	10:30:19	13:31:42	20:30:05	04:30:06
CME speed (km/s)	608	1368	1068	959	977	1645
CME width	191°	H	H	92°	273°	314°
CME acceleration (ms^{-2})	-9.7	+45.6	-36.5	-0.7	-3.3	-77.6
Soft X-ray flare onset (UT)	05:35	13:00[1]	09:53	13:05	20:13	03:54
Soft X-ray flare size	M1.7	M2.4	C7.4	C1.3	C2.8	C9.6
Soft X-ray flare dur. (min)	36	36[1]	54	30	49	41
Soft X-ray flare rise time (min)	18	18[1]	26	15	27	25
H-alpha flare size	1F	SF	SF	?	SF	1F
Flare location	S18E35	S18E15	S15W11	S15W14	S17W29	S14W47
Type III onset at 1 MHz	05:43	13:16	09:51	13:02	20:12	03:57
Type III dur. (14, 1 MHz) (min)	8, 20	11, 16	31, 29	7, 17	25[3], 28	18, 31
Type III peak int. (10^3 sfu)	49.5, 503	326, 53.8	17.8, 40	2.1, 0.5	5.6[3], 42	17, 448
Type III integral int. (10^4 sfu)	15.9, 204	78.3, 26	17.3, 22.4	1.1, 0.8	6.6[3], 28	7.6, 89.3
Type II (freq. range MHz)	95–27	8–0.3	3–0.5	6–3	None	14–0.5
IP shock (m/d hh:mm)	None	4/9 01:47	4/10 19:25	None	None	4/12 17:35
SEP (1.8–3.3 MeV)	?	Yes	Yes	Yes[2]	None	Yes
SEP (26–54 MeV)	None	None	None	None	None	Yes

[1] The GOES profile shows a preceding event. The flare of interest seems to have started at about 13:10 UT as inferred from changes in the SOHO/EIT images.
[2] The CMEs from C3 and C4 are very close, so the SEP event seems to be common to both.
[3] Measurements made at 9 MHz because of the interference at higher frequencies.

we measured the duration at 9 MHz. For other bursts we measured the duration at 14 MHz.

The burst in Fig. 3 and the ones associated with C3 and C6 were of the highest duration, reported in Gopalswamy and Mäkelä (2010).

Figure 4 shows the WAVES/RAD2 dynamic spectra of the three remaining type III bursts associated with C1, C2, and C4. The type III bursts in Fig. 4 are not as spectacular as the others in the AR, but clearly of long duration and complex in the frequency and time axes. The 14 MHz duration is relatively small for the bursts in Fig. 4: the lowest duration is $\sim$7 min for the burst associated with C4. The bursts associated with C1 and C2 had durations of 8 and 11 min, respectively. The 1 MHz durations are larger, the minimum being 16 min for C2 (see Table I). Thus, all the type III bursts satisfy the long-duration criterion ($\geq$ 15 min) used by others (see, e.g., Cliver and Ling, 2009).

Type II Bursts and IP shocks: The CME C1 was accompanied by a metric type II burst (no counterpart in the WAVES data). All other erup-

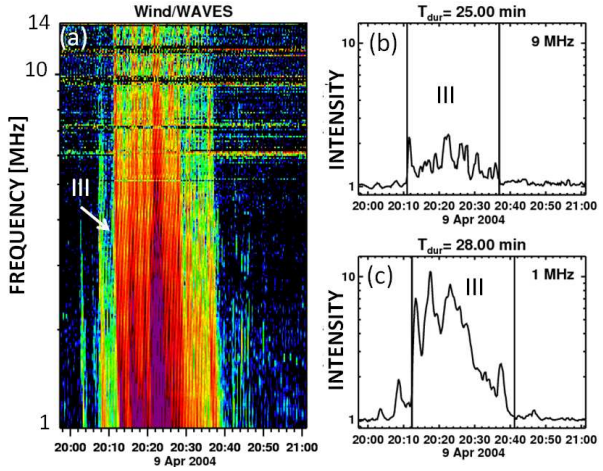

Figure 3: The Wind/WAVES RAD2 dynamic spectrum (a) and the radio intensity with respect to the background at 9 MHz (b) and 1 MHz (c) showing the type III burst duration (T_{dur}) marked by the vertical lines.

tions except C5 were accompanied by type II bursts observed in the WAVES data. The type II bursts associated with C2, C3, and C6 started in the RAD2 spectral range and continued into the RAD1 domain, suggesting that the shocks were strong and propagated far into the IP medium (Gopalswamy et al., 2005). This was confirmed by the detection of the associated IP shocks at L1(Gopalswamy et al., 2010). C1 was accompanied only by a metric type II, which means the CME-driven shock was capable of producing type II emission only near the Sun. The shock did not survive to 1 AU. The type II burst associated with C4 was very brief (6–3 MHz) and the associated shock did not arrive at Earth. Finally, C5 was not associated with an IP shock, consistent with the lack of type II burst.

Radio Flux Density: We also computed the peak and integrated flux densities of the six type III bursts from the WAVES/RAD2 data (1 min resolution) available on line (http://www-lep.gsfc.nasa.gov/waves/waves.html). We follow the calibration procedure given in Dulk et al. (2001) to convert the WAVES data into solar flux units (sfu). The burst flux density $S_b(f)$ at frequency f is given by,

$$S_b(f) = 1.0 \times 10^{22} S_g(f)\{P_b(f)/P_g(f)\} \quad \text{sfu}, \tag{1}$$

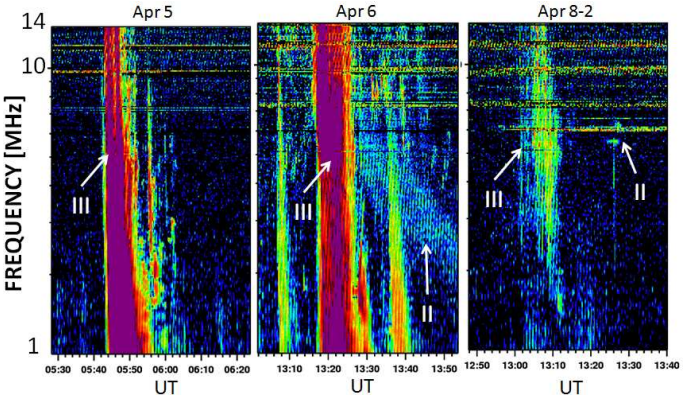

Figure 4: WAVES/RAD2 dynamic spectra (16 s time resolution) showing type III bursts associated with CMEs C1, C2, and C4. The burst on April 6 was associated with a clear type II burst (pointed by an arrow). The type II burst on April 8 was rather brief. This event happened in the aftermath of a previous CME that occurred ∼3 h before (C3).

where $S_g(f)$ is the flux density per beam of the galactic background radiation for a short dipole in free space in the range 0.1 to 30 MHz, and $P_b(f)/P_g(f)$ is the ratio of the burst power to the power of the galactic background radiation. The square root of this quantity is given in the 1 min data files. We computed the peak and integrated flux densities at 14 and 1 MHz using equation (1) with $S_g(14) = 1000$ sfu and $S_g(1) = 398$ sfu obtained from Fig. 1 of Dulk et al. (2001). The flux densities are listed in Table I. The 14 MHz peak (integrated) flux density ranged from 2.1×10^3 sfu (1.1×10^4 sfu) for the second April 8 event to 3.3×10^5 sfu (7.8×10^5 sfu) for the April 6 event. At 1 MHz, the peak (integrated) flux density ranged from 5.0×10^2 sfu (8.5×10^3 sfu) for the C4 event to 5.0×10^5 sfu (2.0×10^6 sfu) for the C1 event. At 1 MHz, the April 5 event had the highest flux density. The 1 MHz flux density calculated using RAD1 data was slightly higher than that from the RAD2 data (RAD1 is connected to a much larger antenna), typically by a factor of ∼4. The 1 MHz integrated flux density obtained from RAD1 data (3.9×10^6 sfu) is consistent with the value 3.02×10^6 obtained by Cliver and Ling (2009) for the April 11 event. In this paper, we use only RAD2 data for comparing with the 14 MHz values, which are available only from RAD2.

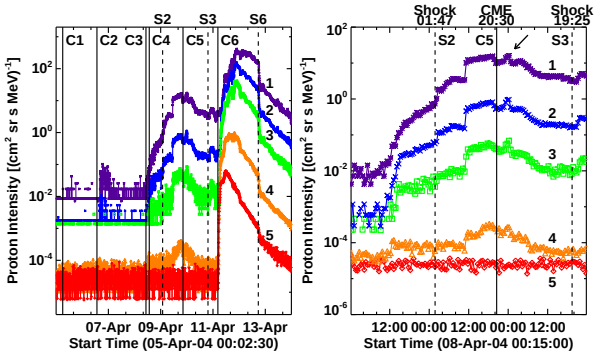

Figure 5: (left) SOHO/ERNE SEP intensity over the interval of interest in several energy channels (1–5). The solid vertical lines mark the first appearance times of the six CMEs (C1-C6). The dashed vertical lines mark the IP shocks S2, S3, and S6, associated with C2, C3, and C6, respectively. The time resolution is 5 min. (right) SEP intensity around C5, the eruption without a type II burst. There was a small spike (pointed by arrow) around 0 UT on April 10 ($\sim$4 h after the appearance of C5). The spike is very short duration ($<$ 2h long) and did not show any dispersion.

3. Solar Energetic Particle Events

Figure 5 shows the time variation of the proton flux observed by SOHO/ Energetic and Relativistic Nuclei and Electron (ERNE; Torsti et al., 1995) experiment in five energy channels (1.8–3.3 MeV, 3.3–6.4 MeV, 6.4–13 MeV, 13–28, and 26–54 MeV) for the period April 5–13, 2004. The first appearance times of the six CMEs and the onset times of 1-AU shocks are also marked on the plot. There are three well-defined SEP events, clearly associated with C2, C3, and C6. The largest peak is associated with C6, which is also a GOES SEP event with a $>$10 MeV intensity of 35 pfu. The second largest peak observed at all channels except the highest energy one. C5 appeared at the time of this peak, but the peak clearly precedes the onset of this CME. This peak appears simultaneously at all energy channels, which suggests that it is due to IP modulation. The third peak after the C2 onset is tiny, appearing only in the two lowest energy channels (1.8–3.3 MeV and 3.3–6.4 MeV). There is also a hint of enhancement following C1 in the lowest energy channel, but its reality cannot be verified. In the highest energy channel (26–54 MeV), there is clearly only one event, associated with C6. C4 occurred when the SEP intensity from C3 is rising, so we cannot say if C4 is associated

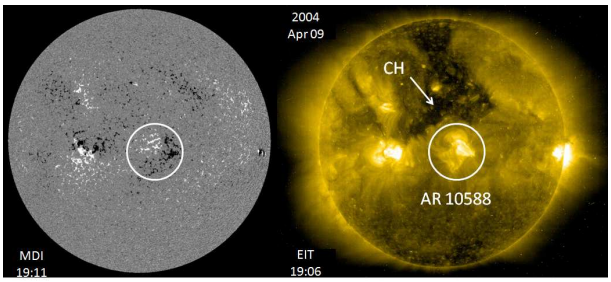

Figure 6: AR 10588 on 2004 April 09 shown circled in the SOHO/MDI magnetogram and in the coronal image from SOHO/EIT at 284 Å. A large coronal hole (CH) can be seen to the north and east of the active region.

with an SEP event above the intensity due to C3. The SEP intensity also shows some changes at the time of the shock arrival at 1 AU. To further confirm the lack of an SEP event associated with C5, we have plotted the SEP intensity over a narrow time range around C5 onset in Fig. 5. One can see a small spike towards the end of the day on April 9—about 4 h after the onset of C5. This spike lasted only for <2 h. Furthermore, the spike peaks at the same time at all energy channels (no event in the highest energy channel), implying IP modulation. Although we cannot rule out the possibility of a weak SEP event in the lower energy channels masked by the event from C3, we can definitely say that there is no event in the 26–54 MeV channel. The lack of an SEP event associated with C5 is remarkable, given that it is a fast and wide CME associated with a long-duration low-frequency type III burst. The lack of SEP event is consistent with the lack of type II emission and IP shock association. C5 is classified as a radio-quiet CME because it lacks type II emission (Gopalswamy et al., 2008a,b; 2010).

4. Active Region Evolution

The active region in question was first observed on 2004 April 1 at a longitude of E74 and rotated behind the west limb on April 14. Table II shows the AR area (in millionths of solar hemisphere, msh), AR longitude at the end of the day, and the magnetic field configuration, all extracted from the data archive available at `http://www.solar.ifa.hawaii.edu/ARMaps/`. The six eruptions shown in Figs. 1 and 2 occurred during April 5–11. The AR area increased by ∼40% before C1 and decreased by a similar amount after

Table II: Area, longitude, and magnetic configuration of AR 10588 in April 2004.

	Date in 2004													
	4/01	4/02	4/03	4/04	4/05	4/06	4/07	4/08	4/09	4/10	4/11	4/12	4/13	4/14
Area	60	60	70	120	170	130	150	140	140	150	90	100	60	40
Longitude	E74	E64	E51	E40	E25	E14	E01	W13	W26	W38	W55	W68	W80	W92
Configuration	α	α	β	β	$\beta\gamma$	β	$\beta\gamma$	β	β	β	β	β	α	α

C6. During the interval of the six eruptions, the AR area remained high in the range 130 to 170 msh and the longitude was in the range E25 to W55. The magnetic configuration of the AR started out as α and became β on April 3 and remained as β or $\beta\gamma$ until the end of April 12. The region was nominally well connected during the second half of the interval in question, when the type III burst associated with C5 occurred.

Figure 6 shows the AR on 2004 April 9, just to the west of the central meridian. The β configuration of the AR is evident from the SOHO/MDI magnetogram. The neutral line is roughly in the north-south direction. Figure 6 and Table I show nothing peculiar about the source active region on April 9 compared to the other days. There was a large coronal hole (CH) to the north and east of the AR, which has been reported to affect the trajectories of CMEs (Gopalswamy et al., 2009b). The AR polarity nearest to the CH was positive, while the CH was of negative polarity. If the coronal hole deflected the CME to the west, it would have made the shock better connected.

5. Is Connectivity an Issue?

If SEPs were accelerated at the same site as the electrons producing the complex type III bursts, then they might follow the same field lines as the type III electrons to the observer. When the eruption region is not well connected to the observer, the electrons propagate along field lines that do not reach Earth, so the lowest frequency at which the type III emission occurs is higher than the local plasma frequency. In such cases, the SEP event maybe seen as slowly increasing or no event at all due to poor connectivity. Is it possible that such a situation prevailed for C5? To check this, we use the Thermal Noise Receiver (TNR) data in the frequency range 4–256 kHz.

Figure 7 shows the TNR dynamic spectrum for the type III bursts as-

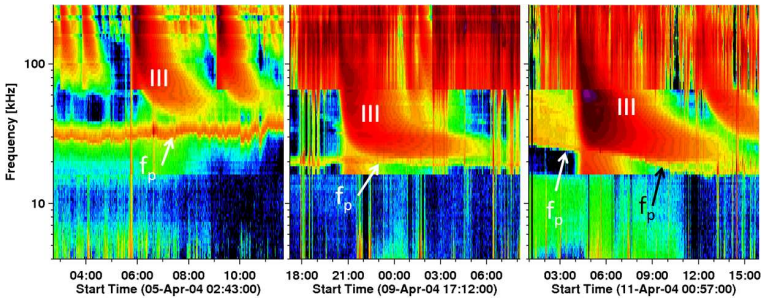

Figure 7: Wind/WAVES TNR dynamic spectra for three type III bursts on April 5, 9, and 11. The plasma line at the Wind spacecraft is marked f_p. Type III burst comes all the way down to the local plasma frequency for the April 9 and 11 bursts. For the April 5 burst, the type III burst is well above the plasma line.

sociated with C1, C5, and C6. C1 occur when the AR was on the eastern hemisphere (see Table II), so it is not well connected to the Wind spacecraft. The local plasma frequency (f_p) was around 30 kHz, but the type III burst occurs at frequencies higher than 40 kHz. This radiation must have occurred at a distance and propagated to Wind. For the type III associated with C5, the emission extends down to the local plasma frequency. The type III burst associated with C6 also extends down to the local plasma frequency, but plasma frequency slowly decreases from ∼30 kHz to 20 kHz over the duration of the type III burst because the density is recovering from the shock compression (S3), which happened at ∼19:25 UT on April 10. Thus, we can conclude that C5 and C6 were well connected, but C1 was poorly connected. Similarly, the type III burst associated with C2 was poorly connected whereas the one associated with C3 was well connected (not shown). The connectivity of the type III burst associated with C4 could not be determined because of the burst from the preceding C3 overlapped. Type III emission at the local plasma frequency suggests that the electron beams propagated all the way to the Wind spacecraft. If SEPs were accelerated along with the electrons, they should have arrived at Earth. We therefore conclude that the lack of an SEP event is not due to poor connectivity.

6. Discussion and Conclusions

We investigated a set of complex type III bursts associated with wide CMEs (width $\geq 60°$) from AR 10588 in April 2004 and examined their SEP as-

sociations. The type III burst on April 9 conspicuously lacked a type II burst and a SEP event, although the type III was of very long duration (28 min at 1 MHz). Three other CMEs from the same AR were associated with SEP events and all of them were accompanied by type II bursts and IP shocks. We conclude that the occurrence of a long-duration type III is not a sufficient condition for a SEP event. This raises an important question regarding the site of particle acceleration. Since there is no shock signature in the April 9 event, it is unlikely that the type III electrons are due to shock acceleration; if the electrons are from the flare reconnection, then why are the protons not accelerated?

It must be pointed out that the CME speed was 977 km/s for the April 9 type III. This is the lowest compared to the other three CMEs accompanied by SEPs: 1368 km/s (C2), 1068 km/s (C3), and 1645 km/s (C6). However, 977 km/s is only 9% lower than the speed of C3, which is associated with a SEP event. This difference is within the CME measurement errors. Then why was the April 9 CME not accompanied by a type II burst? Under the shock-acceleration paradigm, one can explain the lack of type II or SEP event as follows: the April 9 CME must have been injected into a tenuous ambient medium so that it could not drive a shock or the shock was too feeble to accelerate particles. Statistical studies have shown that CMEs as fast as 1600 km/s lacked type II bursts and SEP events (Gopalswamy et al., 2008a,b). Under the flare paradigm, it is difficult to provide such an explanation. The April 9 type III was associated with a C2.8 flare, but even smaller flares are known to be associated with SEP events. Finally, the April 9 event also calls the definition of complex type III burst as "SA (shock-accelerated or shock-associated) event" into question because there is no evidence for shock near the Sun or in the IP medium.

The area and magnetic configuration of AR 10588 remained roughly constant throughout the interval over which the six eruptions occurred. There was nothing peculiar about the conditions in the active region prior to the eruption of the April 9 event. There was a large coronal hole located to the north and east of the AR, but it is not clear if the coronal hole would have selectively affected only one of the eruptions. We also examined the connectivity of the eruption region to the Wind spacecraft using the low-frequency cutoff of the type III bursts. We found that the April 9 type III burst extended down to the local plasma frequency at Wind suggesting that the connectivity was good. Therefore, the lack of SEPs is not due to

poor magnetic connectivity. The only possibility we are left with is that the eruption did not result in SEPs above the detection threshold.

The 1 MHz type III burst flux density and duration are comparable for the April 8 (accompanied by SEPs) and April 9 (lacked SEPs) events. Thus, neither the type III burst duration nor the burst intensity is able to distinguish between SEP and non-SEP events. This result is consistent with Cliver and Ling (2009), who that the complex type III burst intensity did not distinguish between large impulsive and gradual SEP events, but the presence of type II bursts did. These results suggest that the acceleration of low-energy electrons responsible for complex type III bursts at the flare site, does not imply the acceleration of protons.

Acknowledgments: Work supported by NASA's LWS program.

References

Bougeret, J.-L., Kaiser, M. L., Kellogg, P. J., et al.: 1995, *Space Sci. Rev.* **71**, 231.

Cane, H. V., Stone, R. G., Fainberg, J., et al.: 1981, *Geophys. Res. Lett.* **8**, 1285.

Cane, H. V., Erickson, W. C., and Prestage, N. P.: 2002, *J. Geophys. Res.* **107**, 1315.

Cliver, E. W. and Ling, A. G.: 2009, *Astrophys. J.* **690**, 598.

Gopalswamy, N., Kaiser, M. L., Thompson, B. J., et al.: 2000, *Geophys. Res. Lett.* **27**, 1427.

Gopalswamy, N., Aguilar-Rodriguez, E., Yashiro, S., et al.: 2005, *J. Geophys. Res.* **110**, A12S07.

Gopalswamy, N., Yashiro, S., Xie, H., et al.: 2008a, *Astrophys. J.* **674**, 560.

Gopalswamy, N., Yashiro, S., Akiyama, S., et al.: 2008b, *Ann. Geophys.* **26**, 3033.

Gopalswamy, N., Yashiro, S., Michalek, G., et al.: 2009a, *Earth Moon Planets* **104**, 295.

Gopalswamy, N., Mäkelä, P., Xie, H., et al.: 2009b, *J. Geophys. Res.* **114**, A00A22.

Gopalswamy, N. and Mäkelä, P.: 2010, *Astrophys. J.* **721**, L62.

Gopalswamy, N., Xie, H., Mäkelä, P., et al.: 2010, *Astrophys. J.* **710**, 1111.

Kahler, S. W., Cliver, E. W., and Cane, H. V.: 1986, *Adv. Space Res.* **6**, (6)319.

MacDowall, R. J., Lara, A., Manoharan, P. K., et al.: 2003, *Geophys. Res. Lett.* **30**, 8018.

Torsti, J., Valtonen, E., Lumme, M., et al.: 1995, *Sol. Phys.* **162**, 505.

Yashiro, S. and Gopalswamy, N.: 2009, in *Universal Heliophysical Processes*, Proc. IAU Symp. 257, eds. N. Gopalswamy and D. F. Webb, Cambridge University Press, London, pp. 233-243.